

[Ta₆Cl₁₂(PrCN)₆][(Ta₆Cl₁₂)Cl₆]·2PrCN, A Compound with Homonuclear Mixed-Charge Cluster Units [Ta₆Cl₁₂]²⁺ and [Ta₆Cl₁₂]⁴⁺

Nevenka Brničević,^{*,†} Siniša Širac,[†] Ivan Bašić,[†] Zhihong Zhang,[‡] Robert E. McCarley,^{*,‡} and Ilija A. Guzei[‡]

Rudjer Boškovic Institute, Bijenicka 54, 10001 Zagreb, Croatia, and Ames Laboratory, U.S. Department of Energy, and Department of Chemistry, Iowa State University, Ames, Iowa 50011

Received March 18, 1999

Introduction

In transition metal cluster chemistry, compounds consisting of both a cluster cation and a cluster anion are not very common. The first members of this type of compound of the composition [M₆X₁₂(EtOH)₆][(Mo₆Cl₈)Cl₄X₂]·mEtOH·nEt₂O (M = Nb, Ta; X = Cl, Br) have been recently prepared.¹ Crystal structure determinations for [Nb₆Cl₁₂(EtOH)₆][(Mo₆Cl₈)Cl₆]·3EtOH·3Et₂O and [Ta₆Cl₁₂(EtOH)₆][(Mo₆Cl₈)Cl₆]·6EtOH revealed the presence of two different hexanuclear cluster cores; namely, the [M₆X₁₂(EtOH)₆]²⁺ cluster cations and the [(Mo₆Cl₈)Cl₄X₂]²⁻ cluster anions. In fact, these compounds consist of two different heteronuclear cluster units with different charges: [M₆X₁₂]²⁺ in the cation and [Mo₆Cl₈]⁴⁺ in the anion.

The preparation of cation–anion pairs with homonuclear mixed-charge cluster units is also possible. In the present study, the synthesis and crystal structure of the cluster pair [Ta₆Cl₁₂(PrCN)₆][(Ta₆Cl₁₂)Cl₆]·2PrCN is reported. The compound is built of two octahedral homonuclear mixed-charge cluster units: [Ta₆Cl₁₂]²⁺ in the [Ta₆Cl₁₂(PrCN)₆]²⁺ cluster cation and [Ta₆Cl₁₂]⁴⁺ in the [(Ta₆Cl₁₂)Cl₆]²⁻ cluster anion. The phenomenon of different charge states on cation and anion cluster cores has been observed for the first time in the hexanuclear halide cluster chemistry of niobium and tantalum. A preliminary announcement on the crystal structure of this compound was reported at the 18th European Crystallographic Meeting.²

Experimental Section

All manipulations were performed under dry nitrogen atmosphere employing standard Schlenk techniques. The starting cluster (Ta₆Cl₁₂)Cl₂·6EtOH was prepared according to the literature method.³ Absolute ethanol (Kemika) was dried over sodium ethoxide (obtained by dissolving sodium metal), then vacuum distilled and stored over activated 3 Å molecular sieves. Butyronitrile (Aldrich) was dried over P₂O₅ overnight, then vacuum distilled into the flask with activated 3 Å molecular sieves. The IR spectra were obtained as Nujol mulls between CsI plates using a Bomem MB-100 FT IR spectrometer.

Synthesis of [Ta₆Cl₁₂(PrCN)₆][(Ta₆Cl₁₂)Cl₆]·2PrCN. The synthesis of [Ta₆Cl₁₂(PrCN)₆][(Ta₆Cl₁₂)Cl₆]·2PrCN was accomplished in a 100-mL flask, loaded with (Ta₆Cl₁₂)Cl₂·6EtOH (0.5 g, 0.269 mmol) and

Table 1. Crystallographic Data for **1**

empirical formula	C ₃₂ H ₅₆ Cl ₃₀ N ₈ Ta ₁₂	
fw	3787.75	
space group	P1̄	
unit cell dimens	a = 12.1596(7) Å	α = 93.814(1)°
	b = 12.5866(7) Å	β = 93.344(1)°
	c = 13.1720(7) Å	γ = 93.861(1)°
volume, Å ³	2002.92(19)	
Z	1	
D(calcd), g·cm ⁻³	3.140	
μ(Mo Kα), cm ⁻¹	17.340	
temperature, K	163(2)	
R(F), % ^a	2.68	
R(wF ²), % ^a	3.48	

^a Quantity minimized = $R(wF^2) = \sum[w(F_o^2 - F_c^2)^2] / \sum[(wF_o^2)^{1/2}]$; $R = \sum \Delta / \sum (F_o)$, $\Delta = |(F_o - F_c)|$.

PrCN (15 mL), which was vacuum distilled directly into the flask. After being stirred, the reaction mixture became completely clear. At this point, the Schlenk flask was briefly opened and air allowed to enter. Then the flask was closed and left for several months (>6) at ambient conditions. Chunk-like crystals, dark-green in color, were formed together with a significant amount of jelly like material resulting from decomposition of the cluster. The reaction is reproducible with yields of 10 to 15% for crystals isolated by hand picking from the product mixture. IR (Nujol; cm⁻¹): 2285 m, 1303 w, 1265 w, 1155 w, 963 w, 767 w, 324 sh, 319 s, 281 w, 249 s, 242 s, 221 m.

X-ray Structure Determination. An air-sensitive crystal with approximate dimensions 0.18 × 0.16 × 0.11 mm³ was selected under oil at ambient conditions and attached to the top of a glass capillary. The crystal was mounted under a stream of cold nitrogen at 163(2) K and centered in the X-ray beam by using a video camera. The crystal evaluation and data collection were performed on a Bruker CCD-1000 diffractometer with Mo Kα (λ = 0.710 73 Å) radiation and a diffractometer-to-crystal distance of 5.01 cm.

The initial cell constants were obtained from three series of ω scans at different starting angles. Each series consisted of 20 frames collected at intervals of 0.3° in a 6° range about ω with the exposure time of 10 s per frame. A total of 74 reflections was obtained. The reflections were successfully indexed by an automated indexing routine built in the SMART program. The final cell constants were calculated from a set of 6325 strong reflections from the actual data collection.

The data were collected using the hemisphere data collection routine. The reciprocal space was surveyed to the extent of 1.8 hemisphere to a resolution of 0.80 Å. A total of 23 897 data was harvested by collecting four sets of frames with 0.3° scans in ω, with an exposure time of 20 s per frame. These highly redundant data sets were corrected for Lorentz and polarization effects. The absorption correction was based on fitting a function to the empirical transmission surface as sampled by multiple equivalent measurements.⁴

The systematic absences in the diffraction data were consistent for the space groups P1̄ and P1̄.⁵ The E statistics strongly suggested the centrosymmetric choice P1̄, which yielded chemically reasonable and computationally stable results of refinement. A successful solution by the direct methods provided most non-hydrogen atoms from the E map. The remaining non-hydrogen atoms were located in an alternating series of least-squares cycles and difference Fourier maps. All non-hydrogen atoms were refined with anisotropic displacement coefficients. All hydrogen atoms were included in the structure factor calculation at idealized positions and were allowed to ride on the neighboring atoms with relative isotropic displacement coefficients. Both cation and anion are located on inversion centers. There is one butyronitrile solvate molecule present in the asymmetric unit in a general position. This

(4) Blessing, R. H. *Acta Crystallogr.* **1995**, A51, 33–38.

(5) All software and sources of the scattering factors are contained in the SHELXTL (version 5.1) program library (G. Sheldrick, Bruker Analytical X-ray Systems, Madison, WI).

[†] Rudjer Boškovic Institute.

[‡] Ames Laboratory and Department of Chemistry, Iowa State University.

(1) Bašić, I.; Brničević, N.; Beck, U.; Simon, A.; McCarley, R. E. Z. *Anorg. Allg. Chem.* **1998**, 624, 725–732.

(2) Širac, S.; Brničević, N.; Bašić, I.; Planinić, P.; McCarley, R. E. *Bull. Czech Slovak Crystallogr. Assoc.* **1998**, 5, 365.

(3) Kashta, A.; Brničević, N.; McCarley, R. E. *Polyhedron* **1991**, 10, 2031–2036.

Table 2. Selected Bond Distances and Bond Angles for **1**^a

cation		anion	
Bond Distances			
Ta(1)–Ta(2)	2.8753(4)	Ta(4)–Ta(5)	2.9742(4)
Ta(1)–Ta(3)	2.8627(4)	Ta(4)–Ta(6)	2.9767(4)
Ta(2)–Ta(3)	2.8795(4)	Ta(4)–Ta(5)#2	2.9863(4)
Ta(1)–Ta(2)#1	2.8702(4)	Ta(4)–Ta(6)#2	2.9903(5)
Ta(1)–Ta(3)#1	2.8684(4)	Ta(5)–Ta(6)	2.9775(4)
Ta(2)–Ta(3)#1	2.8641(4)	Ta(5)–Ta(6)#2	2.9842(4)
Ta(1)–Cl(1)	2.4567(18)	Ta(4)–Cl(7)	2.4356(18)
Ta(1)–Cl(2)	2.4559(18)	Ta(4)–Cl(8)	2.499(2)
Ta(1)–Cl(4)	2.4529(18)	Ta(4)–Cl(9)	2.4313(19)
Ta(1)–Cl(6)	2.4691(19)	Ta(4)–Cl(13)	2.4162(19)
Ta(2)–Cl(1)#1	2.4611(19)	Ta(4)–Cl(15)	2.4318(19)
Ta(2)–Cl(3)	2.4526(18)	Ta(5)–Cl(9)#2	2.4396(19)
Ta(2)–Cl(4)	2.4550(18)	Ta(5)–Cl(10)	2.4672(19)
Ta(2)–Cl(5)	2.4588(19)	Ta(5)–Cl(11)	2.4250(19)
Ta(3)–Cl(2)#1	2.4520(18)	Ta(5)–Cl(13)	2.4267(19)
Ta(3)–Cl(3)#1	2.4506(17)	Ta(5)–Cl(14)	2.4395(19)
Ta(3)–Cl(5)	2.4700(18)	Ta(6)–Cl(7)#2	2.4357(18)
Ta(3)–Cl(6)	2.4659(19)	Ta(6)–Cl(11)#2	2.4204(19)
Ta(1)–N(1)	2.264(7)	Ta(6)–Cl(12)	2.4951(19)
Ta(2)–N(2)	2.251(6)	Ta(6)–Cl(14)	2.4298(19)
Ta(3)–N(3)	2.245(7)	Ta(6)–Cl(15)	2.4326(19)
Bond Angles			
Ta(3)–Ta(1)–Ta(3)#1	89.963(12)	Cl(13)–Ta(4)–Cl(9)	165.51(7)
Ta(3)–Ta(1)–Ta(2)#1	59.945(10)	Cl(13)–Ta(4)–Cl(15)	88.97(7)
Ta(3)#1–Ta(1)–Ta(2)#1	60.235(11)	Cl(9)–Ta(4)–Cl(15)	88.62(7)
Ta(3)–Ta(1)–Ta(2)	60.241(10)	Cl(13)–Ta(4)–Cl(7)	89.60(7)
Ta(3)#1–Ta(1)–Ta(2)	59.822(10)	Cl(9)–Ta(4)–Cl(7)	89.18(7)
Ta(2)#1–Ta(1)–Ta(2)	90.249(12)	Cl(15)–Ta(4)–Cl(7)	165.56(6)
Cl(4)–Ta(1)–Cl(2)	87.09(6)	Cl(13)–Ta(4)–Cl(8)	82.38(7)
Cl(4)–Ta(1)–Cl(1)	161.17(6)	Cl(9)–Ta(4)–Cl(8)	83.14(7)
Cl(2)–Ta(1)–Cl(1)	88.51(7)	Cl(15)–Ta(4)–Cl(8)	82.47(7)
Cl(4)–Ta(1)–Cl(6)	89.63(6)	Cl(7)–Ta(4)–Cl(8)	83.09(7)
Cl(2)–Ta(1)–Cl(6)	161.37(6)	Cl(11)–Ta(5)–Cl(13)	89.34(7)
Cl(1)–Ta(1)–Cl(6)	88.71(7)	Cl(11)–Ta(5)–Cl(14)	165.80(6)
Cl(3)–Ta(2)–Cl(4)	88.32(6)	Cl(13)–Ta(5)–Cl(14)	89.28(7)
Cl(3)–Ta(2)–Cl(5)	161.63(6)	Cl(11)–Ta(5)–Cl(9)#2	88.13(7)
Cl(4)–Ta(2)–Cl(5)	89.05(7)	Cl(13)–Ta(5)–Cl(9)#2	165.86(7)
Cl(3)–Ta(2)–Cl(1)#1	88.43(7)	Cl(14)–Ta(5)–Cl(9)#2	89.76(7)
Cl(4)–Ta(2)–Cl(1)#1	161.93(6)	Cl(11)–Ta(5)–Cl(10)	83.60(7)
Cl(5)–Ta(2)–Cl(1)#1	88.46(7)	Cl(13)–Ta(5)–Cl(10)	82.28(7)
Cl(3)#1–Ta(3)–Cl(2)#1	88.85(6)	Cl(14)–Ta(5)–Cl(10)	82.21(7)
Cl(3)#1–Ta(3)–Cl(6)	87.80(6)	Cl(9)#2–Ta(5)–Cl(10)	83.62(7)
Cl(2)#1–Ta(3)–Cl(6)	161.07(6)	Cl(11)#2–Ta(6)–Cl(14)	165.62(6)
Cl(3)#1–Ta(3)–Cl(5)	161.33(6)	Cl(11)#2–Ta(6)–Cl(15)	89.36(7)
Cl(2)#1–Ta(3)–Cl(5)	89.03(7)	Cl(14)–Ta(6)–Cl(15)	89.01(7)
Cl(6)–Ta(3)–Cl(5)	88.21(7)	Cl(11)#2–Ta(6)–Cl(7)#2	89.53(7)
N(1)–Ta(1)–Cl(ave)	80.6(2)	Cl(14)–Ta(6)–Cl(7)#2	88.52(7)
N(2)–Ta(2)–Cl(ave)	80.9(2)	Cl(15)–Ta(6)–Cl(7)#2	165.62(6)
N(3)–Ta(3)–Cl(ave)	80.6(2)	Cl(11)#2–Ta(6)–Cl(12)	82.39(7)
		Cl(14)–Ta(6)–Cl(12)	83.23(7)
		Cl(15)–Ta(6)–Cl(12)	82.24(6)
		Cl(7)#2–Ta(6)–Cl(12)	83.41(6)
Angles around Cl Atoms for Both Cation and Anion			
Ta(1)–Cl(1)–Ta(2)#1	71.41(5)	Ta(4)–Cl(7)–Ta(6)#2	75.74(5)
Ta(3)#1–Cl(2)–Ta(1)	71.53(5)	Ta(4)–Cl(9)–Ta(5)#2	75.63(5)
Ta(3)#1–Cl(3)–Ta(2)	71.48(5)	Ta(6)#2–Cl(11)–Ta(5)	76.03(6)
Ta(1)–Cl(4)–Ta(2)	71.72(5)	Ta(4)–Cl(13)–Ta(5)	75.78(5)
Ta(2)–Cl(5)–Ta(3)	71.50(5)	Ta(6)–Cl(14)–Ta(5)	75.39(5)
Ta(3)–Cl(6)–Ta(1)	70.91(5)	Ta(4)–Cl(15)–Ta(6)	75.46(6)

^a Symmetry transformations used to generate equivalent atoms: #1, $-x, -y + 1, -z + 1$; #2, $-x, -y, -z$.

solvate molecule was refined with idealized geometry. Final least-squares refinement of 377 parameters against 8158 data resulted in residuals R (based on F^2 for $I > 2\sigma$) and R_w (based on F^2 for all data) of 0.0268 and 0.0348, respectively. The highest peak (ca. 2.82 eÅ⁻³) in the final difference Fourier map was located 0.92 Å away from atom Ta(5).

A summary of relevant crystallographic data is provided in Table 1, and a list of selected bond distances and angles is given in Table 2.

Results and Discussion

If aliphatic nitriles, RCN, are distilled over (M₆X₁₂)Cl₂·6EtOH (M = Nb, Ta; X = Cl, Br), clear solutions are obtained for R = CH₃.⁶ For R = C₂H₅ or C₃H₇, clear solutions are accessible

(6) Širac, S.; Trojko, R.; Marić, Lj.; McCarley, R. E.; Tolstikhin, O.; Brničević, N. *Croat. Chem. Acta* **1995**, *68*, 905–907.

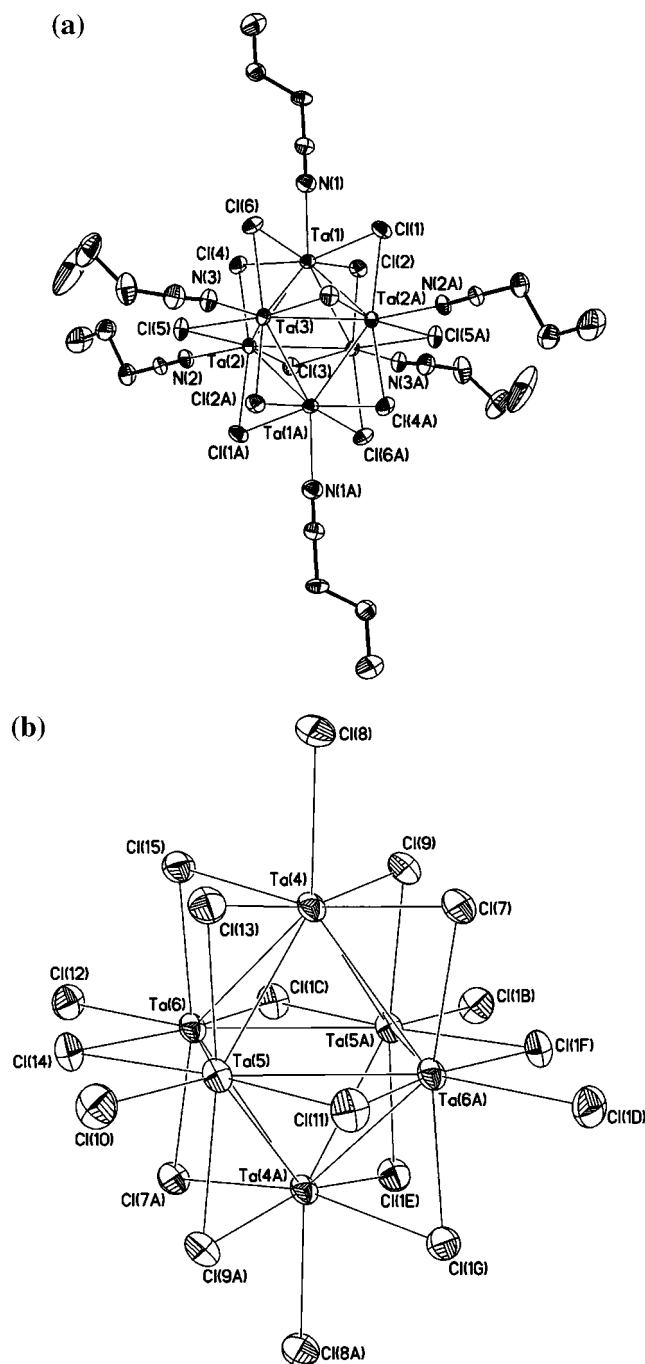


Figure 1. ORTEP drawing for the structure of $[\text{Ta}_6\text{Cl}_{12}(\text{PrCN})_6][(\text{Ta}_6\text{Cl}_{12})\text{Cl}_6] \cdot 2\text{PrCN}$ showing (a) the $[\text{Ta}_6\text{Cl}_{12}(\text{PrCN})_6]^{2+}$ cation and (b) the $[(\text{Ta}_6\text{Cl}_{12})\text{Cl}_6]^{2-}$ anion (50% probability ellipsoids).

only for $(\text{Ta}_6\text{Cl}_{12})\text{Cl}_6 \cdot 6\text{EtOH}$.⁷ From a clear solution of this cluster in butyronitrile, in the presence of a limited amount of oxygen from the air, sufficient for the oxidation of some $[\text{Ta}_6\text{Cl}_{12}]^{2+}$ to $[\text{Ta}_6\text{Cl}_{12}]^{4+}$, chunky green crystals of the composition $[\text{Ta}_6\text{Cl}_{12}(\text{PrCN})_6][(\text{Ta}_6\text{Cl}_{12})\text{Cl}_6] \cdot 2\text{PrCN}$ were formed in 10–15% yield.

In the IR spectrum the absorption band of medium intensity at 2285 cm^{-1} originates from the C–N stretching vibrations of coordinated nitrile ligands. The C–N vibrations from lattice-held PrCN molecules were not observed. The strongest absorption band at 319 cm^{-1} that originates from $\nu(\text{Ta}-\text{Cl}^i)$ (i = inner, bridging) is accompanied by a shoulder at 324 cm^{-1} , which is

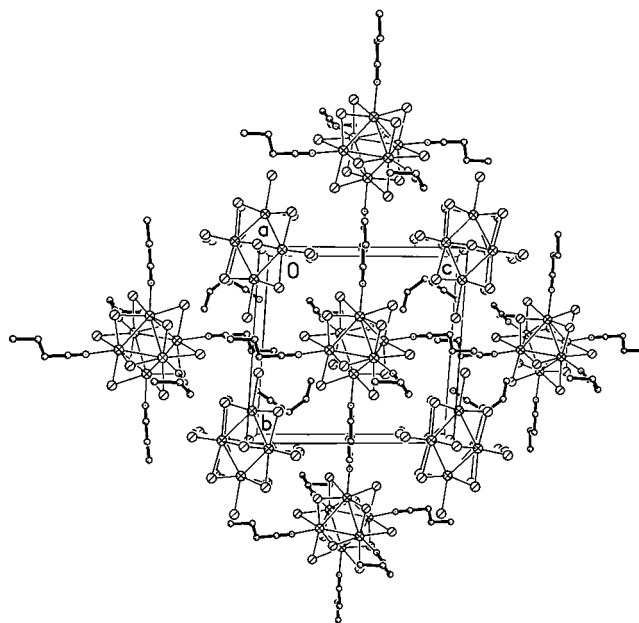


Figure 2. Packing diagram of the title compound viewed down the c axis. Ta and Cl atoms are black and meshed, respectively. N atoms are crossed and C atoms are open circles.

definitely a consequence of the presence of mixed-charge cluster molecules. The shoulder is located at higher wavenumbers and belongs to the stronger Ta–Clⁱ bonds, i.e., to the $[(\text{Ta}_6\text{Cl}_{12})\text{Cl}_6]^{2-}$. The doublet absorption band at 249 and 242 cm^{-1} should correspond to the Ta–Cl^a (a = outside, terminal) stretching vibrations from $[(\text{Ta}_6\text{Cl}_{12})\text{Cl}_6]^{2-}$, since these absorptions are absent in IR spectra of clusters without Cl^a ligands.⁸

$[\text{Ta}_6\text{Cl}_{12}(\text{PrCN})_6][(\text{Ta}_6\text{Cl}_{12})\text{Cl}_6] \cdot 2\text{PrCN}$ crystallizes in the space group $P\bar{1}$. It consists of two octahedral homonuclear cluster units: the $[\text{Ta}_6\text{Cl}_{12}(\text{PrCN})_6]^{2+}$ cation and the $[(\text{Ta}_6\text{Cl}_{12})\text{Cl}_6]^{2-}$ anion (Figures 1 and 2) and two PrCN molecules. The cation and anion have the symmetry $\bar{1}$, imposing for each three crystallographically independent Ta atoms. Twelve edge-bridging chlorine ligands are common to both cluster units (cation and anion), while PrCN molecules and chlorine atoms are ligands in six terminal octahedral coordination sites of the cation and anion, respectively. This is not the only difference between cluster cation and cluster anion. The main difference is in the charges of the two cluster units: the $[\text{Ta}_6\text{Cl}_{12}]^{2+}$ and $[\text{Ta}_6\text{Cl}_{12}]^{4+}$ are present in the $[\text{Ta}_6\text{Cl}_{12}(\text{PrCN})_6]^{2+}$ cluster cation and $[(\text{Ta}_6\text{Cl}_{12})\text{Cl}_6]^{2-}$ cluster anion, respectively. As a consequence of the different oxidation states of tantalum atoms in the $[\text{Ta}_6\text{Cl}_{12}(\text{PrCN})_6]^{2+}$ cation and the $[(\text{Ta}_6\text{Cl}_{12})\text{Cl}_6]^{2-}$ anion, all bond distances (Table 2) in the two octahedral $\text{Ta}_6\text{Cl}_{12}$ units are different. The Ta–Ta bond lengths in $[\text{Ta}_6\text{Cl}_{12}(\text{PrCN})_6]^{2+}$, within the range of $2.8627(4)$ – $2.8795(4)\text{ \AA}$ (average 2.8700 \AA), indicate a slight distortion of the Ta_6 octahedron but are still in the range of distances found for other $(\text{Ta}_6\text{Cl}_{12})^{2+}$ compounds.^{1,9} The Ta–Clⁱ bond distances, in the range of $2.451(2)$ – $2.470(2)\text{ \AA}$ (average 2.458 \AA), are almost identical to the values of other $(\text{Ta}_6\text{Cl}_{12})^{2+}$ members.^{1,9}

The bond distances of the $[(\text{Ta}_6\text{Cl}_{12})\text{Cl}_6]^{2-}$ anion are entirely different from those of the cation. The Ta–Ta bond distances, in the range of $2.9742(4)$ – $2.9903(5)\text{ \AA}$ (average 2.9815 \AA), are longer (0.10 – 0.12 \AA) than those in the cluster cation and are

(8) Fleming, P. B.; Meyer, J. L.; Grindstaff, W. K.; McCarley, R. E. *Inorg. Chem.* **1970**, *9*, 1769–1771.

(9) Imoto, H.; Hayakawa, S.; Morita, N.; Saito, T. *Inorg. Chem.* **1990**, *29*, 2007–2014.

(7) Širc, S. Dissertation, University of Zagreb, Zagreb, Croatia, 1997.

better compared to the same bond distance (2.962(2) Å) in $\text{H}_2[(\text{Ta}_6\text{Cl}_{12})\text{Cl}_6]\cdot 6\text{H}_2\text{O}$, which likewise contains the $(\text{Ta}_6\text{Cl}_{12})^{4+}$ unit.¹⁰ The Ta–Clⁱ bond lengths of 2.416(2)–2.440(2) Å (average 2.430 Å) are shorter than in the cluster cation. As expected, with oxidation of $[\text{Ta}_6\text{Cl}_{12}]^{2+}$ to $[\text{Ta}_6\text{Cl}_{12}]^{4+}$ and loss of two bonding electrons, the Ta–Ta bond distances increase. With increased charge on the cluster unit, the Ta–Clⁱ bond distances decrease. Furthermore, the mean value of the Ta–Cl^a bond distance in the $[(\text{Ta}_6\text{Cl}_{12})\text{Cl}_6]^{2-}$ anion of 2.4871 Å is typical of terminally bonded chlorine atoms.¹⁰

All octahedral coordination sites in the $[\text{Ta}_6\text{Cl}_{12}(\text{PrCN})_6]^{2+}$ cluster cation are occupied by butyronitrile molecules with the Ta–N bond distances ranging from 2.245(7) to 2.264(7) Å (average 2.253 Å). These values fall in the range of M–N bond distances of 1.97(1) or 2.3270(5) Å found for $(\text{CH}_3)_4\text{N}[\text{Pt}(\text{PrCN})\text{Cl}_3]$ ¹¹ or $[\text{Cp}_2\text{Zr}(\text{PrCN})(\mu\text{-OH})_2][\text{BPh}_4]\cdot 4\text{PrCN}$,¹² respectively. The mean value for the N–C bond distance from coordinated PrCN of 1.134 Å, as well as the Ta(1)–N(1)–C(1) or Ta(2)–N(2)–C(5) angles of 175(7)° and 170(7)°, respectively, correlate well with the data observed for $(\text{CH}_3)_4\text{N}[\text{Pt}(\text{PrCN})\text{Cl}_3]$ (1.13(2) Å and 174(1)°).¹² The C–C bond distances in the coordinated PrCN molecules, in the range of 1.458(10)–1.535(12) Å, and the associated bond angles are typical of coordinated, σ -bonded butyronitrile. In addition, two solvent molecules (PrCN) are located between the cluster layers parallel to the [011] direction.

When the $[\text{Ta}_6\text{Cl}_{12}\text{L}_6^a]^{4+}$ unit is terminally ligated with oxygen donor ligands (L^a), the geometry of the cluster is dependent on the nature of the oxygen donor atoms and the particular hydrogen bonding system involved. Usually, the shortest Ta–O^a bonds are associated with long Ta–Ta bond distances.¹³ In the absence of any hydrogen bonds involving N atoms from coordinated PrCN molecules, as well as in the presence of only very weak intermolecular contacts involving crystalline PrCN [N(4)···H(10c)–C(10)#1 of 3.337 Å], the interatomic distances observed for the title compound represent the geometry for $[\text{Ta}_6\text{Cl}_{12}]^{2+}$ and $[\text{Ta}_6\text{Cl}_{12}]^{4+}$ units free of the influence of hydrogen bonding effects. If hydrogen bonding was of any significance here, an elongation of the Ta(3)–N(3) bond distance of 2.245(7) Å would occur. On the contrary, this distance is the shortest one compared to the other values of 2.264(7) and 2.251(6) Å listed in Table 2.

Acknowledgment. The financial support of the Ames Laboratory, operated for the U.S. Department of Energy by Iowa State University under Contract No. W-7405-Eng-82; the Joint U.S.–Croatia Board on Scientific and Technological Cooperation (Contract JF 104); and the Ministry of Science and Technology of the Republic of Croatia (Project 980908) is gratefully acknowledged.

Supporting Information Available: Complete tables of crystallographic data, all atomic positional and isotropic thermal parameters, anisotropic thermal parameters for all non-hydrogen atoms, and bond distances and angles. This material is available free of charge via the Internet at <http://pubs.acs.org>.

IC9903073

- (10) Thaxton, C. B.; Jacobson, R. A. *Inorg. Chem.* **1971**, *10*, 1460–1463.
(11) Rochon, F. D.; Melanson, R.; Thouin, E.; Beauchamp, A. L.; Bensimon, C. *Can. J. Chem.* **1996**, *74*, 144–152.
(12) Aslan, H.; Eggers, S. H.; Fischer, R. D. *Inorg. Chim. Acta* **1989**, *159*, 55–57.

- (13) Beck, U.; Simon, A.; Širac, S.; Brničević, N. Z. *Anorg. Allg. Chem.* **1997**, *623*, 59–64.